Revealing the competitive dynamics of influenza viruses through evolutionary cartography

Trevor Bedford[1], Marc A. Suchard[2,3,4], Philippe Lemey[5], Gytis Dudas[1], Colin Russell[6], Derek Smith[6,7] & Andrew Rambaut[1,8]

[1]Institute of Evolutionary Biology, University of Edinburgh, Edinburgh, UK
[2]Department of Biomathematics, David Geffen School of Medicine at UCLA, University of California, Los Angeles CA, USA
[3]Department of Human Genetics, David Geffen School of Medicine at UCLA, University of California, Los Angeles CA, USA
[4]Department of Biostatistics, UCLA School of Public Health, University of California, Los Angeles CA, USA
[5]Department of Microbiology and Immunology, Katholieke Universiteit Leuven, Leuven, Belgium
[6]Department of Zoology, University of Cambridge, Cambridge, UK.
[7]Department of Virology, Erasmus Medical Centre, Rotterdam, Netherlands.
[8]Fogarty International Center, National Institutes of Health, Bethesda, MD, USA.

Abstract

Influenza viruses undergo continual antigenic evolution allowing mutant viruses to evade immunity acquired by the host population to previous virus strains. However, the extent to which antigenic evolution determines competitive dynamics within and between virus clades A/H3N2, A/H1N1, B/Victoria and B/Yamagata has remained unclear. Here, we develop a novel cartographic approach to simultaneously characterize the genetic and antigenic evolution of viral lineages. Through this approach, we determine historical rates and patterns of antigenic drift in all four viral clades and we show that antigenic drift influences year-to-year variability in clade dominance. We investigate the selective underpinnings for differing antigenic dynamics across clades and suggest that pleiotropic effects linked to antigenic mutation determine selective outcomes.

Introduction

Seasonal influenza infects between 10% and 20% of the human population every year, causing 250,000 to 500,000 deaths annually [1]. While individuals develop long-lasting immunity to particular influenza strains after infection, antigenic mutations to the influenza virus genome result in proteins that are recognized to a lesser degree by the human immune system, leaving individuals susceptible to future infection. The influenza virus population

continually evolves in antigenic phenotype in a process known as antigenic drift. A large proportion of the disease burden of influenza stems from antigenic drift; it is why vaccines remain only transiently effective. A thorough understanding of the process of antigenic drift is essential to our efforts to control mortality and morbidity through the use of a seasonal influenza vaccine.

Before 2009, there were four major clades of influenza circulating within the human population: influenza A H3N2 and H1N1, and influenza B Victoria and Yamagata. In the case of influenza A, subtypes A/H3N2 and A/H1N1 refer to the genes, hemagglutinin (H or HA) and neuraminidase (N or NA), that are primarily responsible for the antigenic character of a strain. In the case of influenza B, B/Vic and B/Yam refer to antigenically distinct lineages which diverged from one prior to 1980 [2]. Mutations to the HA1 region of the hemagglutinin protein are thought to drive the majority of antigenic drift in the influenza virus [3]. Experimental characterization of antigenic phenotype is possible through the hemagglutination inhibition (HI) assay [4], which measures the cross-reactivity of one virus strain to serum raised against another strain through challenge or vaccination. Sera from older strains react poorly with more evolved viruses resulting in new strains having a transmission advantage over established strains. HI assays have shown there to be little to no cross-reactivity between influenza clades A/H3N2, A/H1N1, B/Vic and B/Yam [5].

The results of many HI assays across a multitude of virus strains can be combined to yield a two-dimensional map, quantifying antigenic similarity and distance [6]. The antigenic map of influenza A (H3N2) has shown largely linear movement of the influenza virus population since its introduction in 1968. Evolution of antigenic phenotype appears punctuated with periods of stasis interspersed by periods of more rapid innovation, while genetic evolution appears more continuous [6], suggesting that a relatively small number of genetic changes or combinations of genetic changes may drive changes in antigenic phenotype. The process of antigenic drift results in the rapid turnover of the virus population. Although mutation occurs rapidly, standing genetic diversity is low and phylogenetic analysis shows a characteristically 'spindly' tree with a single predominant trunk lineage and transitory side branches that persist for only 1–5 years [7].

Previously, the antigenic and genetic patterns of influenza evolution have been analyzed essentially in isolation. An antigenic map is constructed from a panel of HI measurements, and a phylogenetic tree is constructed from sequence data. However, the opportunity for a combined approach exists as both the antigenic map and the phylogenetic tree often contain many of the same isolates. Here, we implement a flexible Bayesian approach to jointly characterize the antigenic and genetic evolution of the influenza virus population. We apply this approach to investigate the dynamics of clades A/H3N2, A/H1N1, B/Vic and B/Yam.

Results and Discussion

Antigenic and evolutionary cartography

In order to assess patterns of antigenic evolution among influenza strains, we implemented a Bayesian probabilistic analog of multidimensional scaling, referred to here as BMDS (see Methods). In this model, viruses and sera are given N-dimensional locations, thus specifying an 'antigenic map', such that distances between viruses and sera in this space are inversely proportional to cross-reactivity. In the BMDS model, a map distance of one antigenic unit translates to an expectation of a 2-fold drop in HI titer between virus and sera. Maps that produce pairwise distances most congruent with the observed titers will have a high likelihood and will be favored by the BMDS model. We integrate over sources of uncertainty, such as antigenic locations, in a flexible Bayesian fashion. We apply this model to HI measurements of virus isolates against post-infection ferret sera for influenza A/H3N2, A/H1N1, B/Vic and B/Yam (see Methods).

We test model performance by constructing a training dataset representing 90% of the HI measurements of the A/H3N2 dataset and a test dataset representing the remaining 10% of the full dataset. By fitting the BMDS model to the training dataset, we are able to predict HI titers in the test dataset and compare predicted titers to observed titers in the test dataset. We find that a BMDS analog of the model used by Smith et al. [6], in which viruses and sera are represented as 2D locations and expected titer is relative to the maximum titer of a particular ferret sera, performs well, yielding an average absolute predictive error of 0.87 $\log_2$ HI titers (Table 1). We find that a model with two dimensional antigenic locations predicts test data to the same precision as a 3D model, but performs substantially better than a 1D model or models with four or more dimensions (Table 1), and thus specify a two dimensional model in all subsequent analyses. We extend this model by estimating the strength of overall reactivity of each serum rather than fixing this at the maximum titer, and additionally, by estimating the strength of reactivity of each virus isolate. We refer to these estimates as serum effects and virus effects, respectively. We found that including these effects decreased test error to 0.75 for influenza A/H3N2. We arrive at similar precisions when repeating this analysis for A/H1N1, B/Vic and B/Yam. For the 2D model with serum and virus effects, A/H1N1 shows a test error of 0.64, B/Vic shows a test error of 0.74 and B/Yam shows a test error of 0.80.

Table 1. Absolute prediction error of $\log_2$ HI titer against A/H3N2 test data across models.

BMDS dimension	Serum effects	Virus effects	Test error
1D	Fixed	None	1.05
2D	Fixed	None	0.87
3D	Fixed	None	0.87
4D	Fixed	None	0.91
5D	Fixed	None	0.97
2D	Estimated	None	0.78
2D	Estimated	Estimated	0.75

Most previous work on virus antigenic and genetic evolution has examined antigenic and genetic patterns in isolation, and then compared the results to assess congruence of these two aspects of evolution [5, 6, 8]. Here, we simultaneously model antigenic and genetic evolution by adapting an evolutionary diffusion process [9], wherein a virus's antigenic character state evolves along branches of phylogenetic tree according to Brownian motion process (see Methods). Here, the diffusion process acts as a prior, so that genetically similar viruses are expected to share similar antigenic phenotypes, and we model the relationship between genetic change and accrual of antigenic distance. We include sequence data for A/H3N2, A/H1N1, B/Vic and B/Yam to estimate this diffusion process. We find similar levels of predictive accuracy when including the diffusion process with A/H3N2 showing a test error of 0.75, A/H1N1 showing a test error of 0.66, B/Vic showing a test error of 0.70 and B/Yam showing a test error of 0.78.

Antigenic evolution across influenza lineages

Through our modeling, we reveal the evolutionary basis for antigenic phenotype in influenza A/H3N2, A/H1N1, B/Vic and B/Yam (Figure 1). Over the time period of 1968 to 2011, influenza A/H3N2 shows substantially more antigenic evolution than is exhibited by A/H1N1 over the course of 1977 to 2009 or B/Vic and B/Yam over the course of 1986 to 2011. We observe prominent antigenic clusters in A/H3N2 and A/H1N1 with less obvious clustering in B/Vic and B/Yam. Antigenic clusters show high genetic similarity, so that we only observe a single diffusion event leading to each cluster, rather than the repeated emergence of clusters. This analysis makes the fate of antigenic clusters obvious, with two clusters in A/H3N2 (Texas/77 and Beijing/89) appearing to be evolutionary dead-ends.

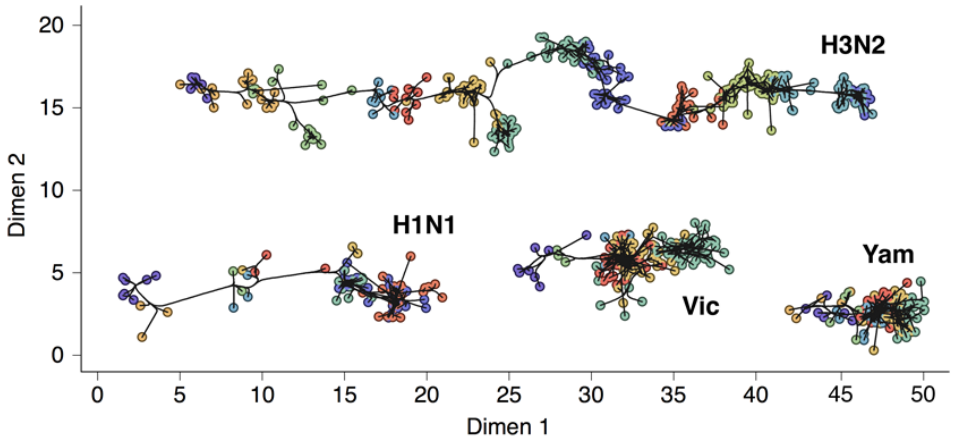

Figure 1. Antigenic locations of A/H3N2, A/H1N1, B/Vic and B/Yam viruses showing evolutionary relationships between virus samples. Circles represent a posterior sample of virus locations and have been colored based on year of isolation in 4-year intervals. Antigenic units represent two-fold dilutions of the HI assay. Distances between clades, e.g. A/H3N2 and A/H1N1, are arbitrary. Lines represent mean posterior diffusion paths when virus locations are fixed.

HI assays lack sensitivity beyond a certain point, so that for A/H3N2, cross-reactive mea-

surements only exist between strains sampled at most 11 years apart, leaving only threshold titers, e.g. '<40', in more temporally distant comparisons. Because of the threshold of sensitivity of the HI assay, it's impossible to distinguish a linear trajectory in 2D antigenic space, from a curved trajectory, so long as the curve does not bring antigenic phenotype full circle to have cross-reactive measurements between temporally distant strains. To solve this problem of identifiability, we assumed a weak prior that favors linear movement in the 2D antigenic space, with the slope of the linear relationship and the precision of the relationship incorporated into the Bayesian model (see Methods). Because of this, we interpret antigenic locations locally rather than globally. We can determine the rate of antigenic movement of virus lineages without knowing the larger configuration that the movement occurs under.

We find that influenza A/H3N2 evolved along antigenic dimension 1 at a rate of 1.00 antigenic units per year, with a 95% highest posterior density (HPD) interval of 0.97–1.04 (Figure 2). However, the rate of antigenic drift was not constant, with year-to-year movement of mean antigenic phenotype showing an interquartile range of 0.00–1.57. Large jumps in antigenic phenotype (Figure 2) correspond to cluster transitions identified by Smith et al. [6]. Most variation is contained within the first antigenic dimension, but dimension 2 occasionally shows variation when two antigenically distinct lineages emerge and transiently coexist (Figure 1), as is the case with the previously identified Beijing/89 and Beijing/92 clusters.

We find that other clades of influenza evolved in antigenic phenotype substantially slower than A/H3N2 (Figure 2). Influenza A/H1N1 evolved at a rate of 0.55 antigenic units per year (HPD 0.49–0.62), but showing a similar pattern of punctuated antigenic evolution with occasional larger jumps in phenotype, such as the emergence of the Solomon Islands/06 cluster. Influenza B/Victoria also evolved relatively slowly, with an average rates of 0.41 (HPD 0.29–0.55) antigenic units per year. Influenza B/Vic appears to show some degree of punctuated antigenic evolution with a recent transition creating the Brisbane/08 cluster. Interestingly, a minor lineage of B/Vic has persisted that rather than moving forward on antigenic dimension 1 has moved down on antigenic dimension 2 (Figure 1, Figure 2). Influenza B/Yamagata evolves slower still, with an average rate of and 0.21 (HPD 0.10–0.28) antigenic units per year. Very little punctuated evolution is apparent in the evolution of B/Yam.

Competition between influenza clades

We investigated the relative rates of antigenic evolution in different influenza lineages from 1999 to 2009, finding a general correspondence between antigenic drift along antigenic dimension 1 and relative incidence between influenza A/H3N2, A/H1N1, B/Vic and B/Yam. From 1999 to 2009, influenza A (H3N2) accounted for the majority of antigenic evolution (51%), while A/H1N1, B/Vic and B/Yam split the remainder, accounting for 17%, 18% and 14%, respectively. Similarly, influenza A (H3N2) was responsible for the majority of incidence (54%) in the USA during this time period. Influenza A (H1N1) accounted for 23% of incidence, B/Vic accounted for 12% of incidence and B/Yam accounted for 10% of incidence. These proportions are significantly similar to one another (randomization test

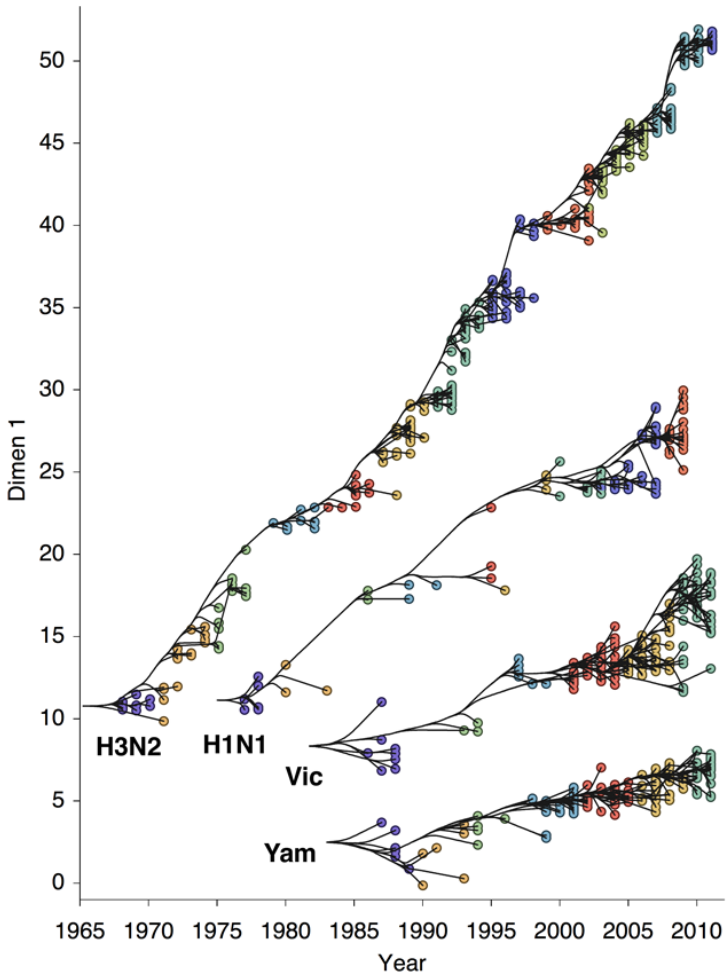

Figure 2. Antigenic drift of A/H3N2, A/H1N1, B/Vic and B/Yam viruses showing evolutionary relationships between virus samples. Antigenic drift is shown in terms of change of location in the first antigenic dimension through time. Circles represent a posterior sample of virus locations and have been colored based on year of isolation in 4-year intervals. Antigenic units represent two-fold dilutions of the HI assay. Distances between clades, e.g. A/H3N2 and A/H1N1, are arbitrary. Lines represent mean posterior diffusion paths when virus locations are fixed.

$p = 0.010$).

Methods

Bayesian multidimensional scaling

Antigenic characteristics of viral strains are often assessed through immunological assays such as hemagglutination inhibition (HI) [4]. At heart, these assays compare the reactivity H_{ij} of one virus strain i to antibodies raised against another virus strain j via challenge or

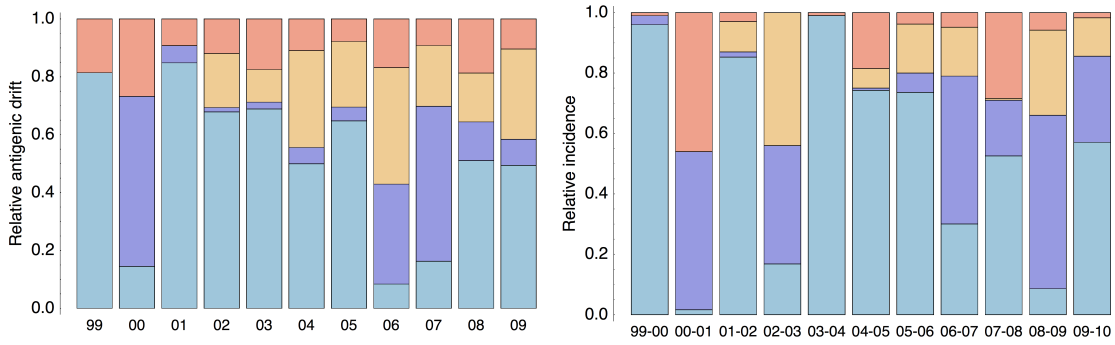

Figure 3. Relative antigenic drift and incidence between lineages of influenza from 1999 to 2009. (A) Relative antigenic drift of influenza A H3N2 and H1N1 and influenza B Victoria and Yamagata lineages. Relative change in antigenic dimension 1 between year i and year $i-1$ is shown for each of the 4 lineages. (B) Relative incidence of influenza A H3N2 and H1N1 and influenza B Victoria and Yamagata lineages. Relative isolation counts of each lineage in the USA for each winter influenza season.

vaccination. In the case of HI, the measurement of cross-reactivity takes the form of a titer representing the dilution factor at which serum raised against virus j ceases to be effective at inhibiting binding of virus i. These factors are commonly assessed by serial dilution, so that HI titers will form a log series, 40, 80, 160, etc .... However, due to experimental constraints, most comparisons cannot be made, leading to a sparse observation matrix $\mathbf{H} = \{H_{ij}\}$. Further, measurements are usually interval and truncated, e.g. inhibition or neutralization may cease somewhere between the serial titers of 160 and 320, or inhibition or neutralization may be absent at all titers assayed, suggesting a threshold somewhere between 0 and 40.

Previous work [6, 10] has used multidimensional scaling to place viruses and sera on an 'antigenic map'. These methods heuristically optimize locations of viruses and sera by seeking to minimize the sum of squared errors between titers predicted by map locations and observed titers. Antigenic maps produced by these methods have proved useful in categorizing virus phenotypes [6], but the extension of these methods to integrate genetic data has not yet been attained.

Here, we follow previous models in representing antigenic locations as points in an N-dimensional antigenic map. Our goal is to find an optimal projection of the high-dimensional distance matrix $\mathbf{H}$ into a lower number of dimensions. We conduct this projection using Bayesian multidimensional scaling (BMDS) [11] in which a probabilistic model is constructed to quantify the fit of a particular configuration of cartographic locations to the observed matrix of serological measurements.

Let $X_i \in \Re^P$ represent the cartographic location of virus i for $i = 1, \ldots, n$, and Y_j represent the cartographic location of serum j for $j = 1, \ldots, k$. Virus and antiserum may be isolated from / raised against the same strain and have different cartographic locations. Typically, $P = 2$, but higher or lower dimensions may better reflect the data. This gives set of distances between virus and serum cartographic locations

$$\delta_{ij} = ||X_i - Y_j||_2. \tag{1}$$

Here, H_{ij} represents the $\log_2$ titer of virus i against serum j, and immunological distance can be defined as

$$d_{ij} = S_j - H_{ij}, \tag{2}$$

where $S_j = \max(H_{1j}, \ldots, H_{nj})$. Traditionally, the goal of multidimensional scaling (MDS) optimizes over $\mathbf{X}$ and $\mathbf{Y}$ such that

$$\sum_{(i,j)\in\mathcal{I}} (\delta_{ij} - d_{ij})^2 \tag{3}$$

is minimized, where $\mathcal{I} = \{(\rangle, |) : \mathcal{H}_{\rangle|} \text{ is measured}\}$. Here, we instead assume a probabilistic interpretation in which an observed titer is normally distributed around its cartographic expectation

$$H_{ij} \sim \text{Normal}(S_j - \delta_{ij}, \varphi^2), \tag{4}$$

and the likelihood of observing a particular titer given the placement of antigenic locations is

$$f_|(H_{ij}) = \phi\left(\frac{H_{ij} + \delta_{ij} - S_j}{\varphi}\right), \tag{5}$$

where φ^2 represents variance and $\phi(\cdot)$ represents the standard normal PDF. HI assays sometimes show no inhibition at all measured titrations, e.g. a measurement can be reported as '<40'. In this case, the likelihood of observing the threshold measurement follows the cumulative density of the lower tail of the normal distribution

$$f_\lrcorner(H_{ij}) = \Phi\left(\frac{H_{ij} + \delta_{ij} - S_j}{\varphi}\right), \tag{6}$$

where $\Phi(\cdot)$ represents the standard normal CDF. Although it is simplest to assume that immunological measurements represent point estimates, it seems more natural to assume that the threshold for inhibition occurs between two titers, e.g. we observe inhibition at 1:40 dilution and no inhibition at 1:80 dilution. Rather than taking the HI titer as 40, we can instead treat this as an interval measurement, assuming that the exact titer for inhibition would occur somewhere between 40 and 80. HI titers are usually reported as the highest titer that successfully inhibits virus binding or growth, so that in this case, we calculate the likelihood of an interval measurement as

$$f_\sqcup(H_{ij}) = \Phi\left(\frac{H_{ij} + \delta_{ij} - S_j + 1}{\varphi}\right) - \Phi\left(\frac{H_{ij} + \delta_{ij} - S_j}{\varphi}\right). \tag{7}$$

These likelihoods are illustrated in Figure 4. Throughout our analyses, we use interval likelihoods $f_\sqcup$ rather than point likelihoods $f_|$ unless otherwise noted.

We calculate the overall likelihood by multiplying probabilities of individual measurements

$$L(\mathbf{X}, \mathbf{Y}) = \prod_{(i,j)\in\mathcal{I}} f(H_{ij}), \tag{8}$$

using probability functions $f_|$, $f_\lrcorner$ and $f_\sqcup$ as appropriate. We assume that the prior precision $1/\varphi^2$ follows a diffuse Gamma(a, b) distribution with $a = 0.001$ and $b = 1000$, and we start by assuming a diffuse normal prior Normal(μ, Σ) over virus and sera locations $\mathbf{X}$

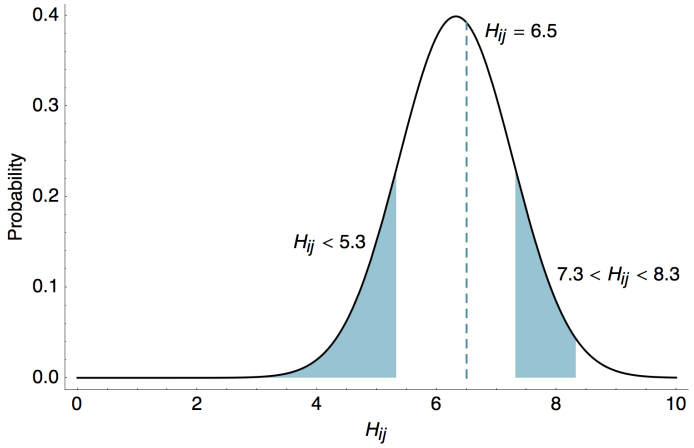

Figure 4. Likelihood of HI titers in the BMDS model. Here we show the likelihoods of observing three different outcomes given $\delta_{ij} = 4$, $\varphi = 0.95$ and $S_j = \log_2 1280 = 10.32$. The likelihood of observing a threshold titer of '<40' is equal to the lower tail of the probability density function $f_{\lrcorner}(5.32) = 0.146$. The likelihood of observing a point measurement with an exact inhibiting titer of '90.5' is equal to the density function $f_{|}(6.5) = 0.413$. The likelihood of observing an interval measurement with an inhibiting titer somewhere between '160' and '320' is equal to $f_{\sqcup}(7.32) = 0.129$.

and $\mathbf{Y}$, where μ is equal to $\{0, 0\}$ and Σ is equal to 1000 along diagonal entries and equal to zero along off-diagonal entries.

We integrate over uncertainty using the Markov chain Monte Carlo (MCMC) procedures implemented in the phylogenetic package BEAST [12]. Metropolis-Hastings proposals include moves to individual virus and serum locations X_i and Y_j, scaling of the entire set of virus and serum locations $\mathbf{X}$ and $\mathbf{Y}$ and scaling φ.

Incorporating virus and serum effects

The preceding model represents immunological distance as a drop in titer against the most reactive comparison for a particular antiserum. Here, we relax this assumption and treat the maximum reactivity of a sera as a random variable. In this case, H_{ij} still follows

$$H_{ij} \sim \text{Normal}(S_j - \delta_{ij}, \varphi^2), \tag{9}$$

but the vector of 'serum effects' $\mathbf{S}$ is estimated rather than fixed. We assume that S_j values are hierarchically distributed according to a normal distribution. The mean and variance of this distribution is taken from the empirical mean and empirical variance of the set of maximum titers across sera $\{\max(H_{1j}, \ldots, H_{nj}) : j = 1, \ldots, k\}$. This formulation assumes that particular sera are more reactive in general than other sera.

Additionally, we follow the same logic and assume that particular virus isolates are more reactive in general than other virus isolates. With virus reactivity included, H_{ij} follows

$$H_{ij} \sim \text{Normal}\left(\frac{V_i + S_j}{2} - \delta_{ij}, \varphi^2\right), \tag{10}$$

and the vector of 'virus effects' V_i for $i = 1, \ldots, n$ is estimated in an analogous hierarchical fashion, with $\mathbf{V}$ normally distributed with mean and variance equal to the empirical mean and variance of the set of maximum titers across viruses $\{\max(H_{i1}, \ldots, H_{ik}) : i = 1, \ldots, n\}$.

With these effects included, Metropolis-Hastings proposals additionally incorporate moves to individual serum effects S_j and virus effects V_i.

Antigenic drift prior

As presented, virus and serum locations $\mathbf{X}$ and $\mathbf{Y}$ accurately characterize antigenic distances between virus strains based on titers from pairwise HI assays. However, these distances represent only a local description of antigenic space and do not provide a global picture. An example of this phenomena is shown in Figure 5. In this case it is impossible to determine from the HI data at hand whether the blue and yellow viruses are antigenically similar or antigenically divergent. This presents an issue of model identifiability; multiple antigenic maps give the same likelihood of observing the serological data. In order to achieve more interpretable antigenic locations we impose a weak prior on global locations. In influenza, it's clear that antigenic distance between strains increases with time [6, 10]. To capture this, we replace the diffuse normal prior on virus locations with a prior in which virus locations are distributed according to a multivariate normal distribution in which the expectation of the first antigenic dimension increases according to date of virus sampling

$$X_i \sim \text{Normal}(\{\beta\, y_i, 0\}, \Sigma) \tag{11}$$

for $P = 2$, where y_i is the difference in time between virus i and the earliest sampled virus and covariance matrix Σ is equal to ϑ^2 along diagonal entries and equal to zero along off-diagonal entries. Thus, this model assumes that the virus population drifts in a line across the antigenic map at rate β. The parameter ϑ determines the breadth of the virus population at each point in time. We assume that both the prior slope β and the prior precision $1/\vartheta^2$ follow a diffuse Gamma(a, b) distribution with $a = 0.001$ and $b = 1000$. We further introduce Metropolis-Hastings proposals that scale β and ϑ.

Diffusion model of antigenic evolution

We simultaneously model antigenic locations and genetic relatedness by assuming that viruses diffuse across the antigenic map according to a Brownian motion process [9]. To do this, we incorporate a prior on virus locations according to the evolutionary process

$$(X_1, \ldots, X_n) \sim \text{Evolutionary Brownian Process}(\tau, \sigma), \tag{12}$$

where τ is a phylogeny specifying tree topology and branch lengths and σ is the volatility parameter of the Brownian motion, set to have equal variance in each antigenic dimension and no correlation across dimensions. Thus, viruses which are genetically similar are induced to have prior locations close to one another on the antigenic map. The phylogenetic tree τ is estimated using sequence data for viruses $1, \ldots, n$ according to well established methods implemented in the software package BEAST [12]. The volatility parameter σ is

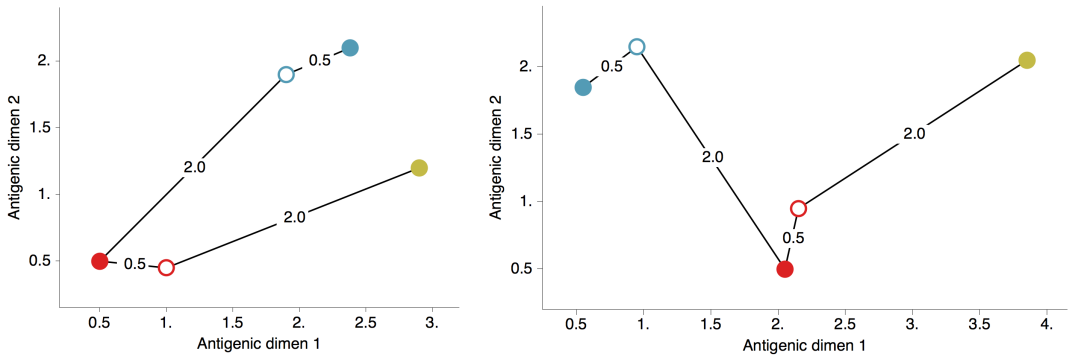

Figure 5. Schematic antigenic map with three viruses and two sera. Virus 1 is shown in blue, virus 2 is shown in red and virus 3 is shown in yellow. Virus isolates are represented by filled circles, sera raised against viruses are shown as open circles and map distances δ_{ij} are shown as solid lines connecting viruses and sera. Sera from virus 1 is compared against viruses 1 and 2, while sera from virus 2 is compared against viruses 1 and 3. Left and right panels represent cartographic models that would give equal likelihoods of a given set of serological data $\{H_{11}, H_{21}, H_{22}, H_{32}\}$.

estimated jointly from the genetic and antigenic data. Parameter σ is assumed to follow a diffuse Gamma(a, b) distribution with $a = 0.001$ and $b = 1000$. Metropolis-Hastings proposals scale σ. The probability of observing virus locations $p(\mathbf{X}|\tau, \sigma)$ is determined through analytical integration across internal states following the methods introduced in [9]. Thus, under the full model, the posterior probability of observing virus and serum locations given immunological data and phylogeny is factored

$$p(\mathbf{X}, \mathbf{Y}|\mathbf{H}, \tau) = \frac{p(\mathbf{H}|\mathbf{X}, \mathbf{Y}, \mathbf{S}, \mathbf{V}, \varphi)\; p(\mathbf{X}|\beta, \vartheta)\; p(\mathbf{X}|\tau, \sigma)\; p(\mathbf{Y}, \mathbf{S}, \mathbf{V}, \varphi, \beta, \vartheta, \sigma)}{p(\mathbf{H})}. \qquad (13)$$

Genetic and antigenic data

We compiled an antigenic dataset of hemagglutination inhibition (HI) measurements of virus isolates against post-infection ferret sera for influenza A (H3N2) by collecting data from previous publications [5, 6, 8, 13], NIMR vaccine strain selection reports for 2002 and 2008–2012 [14–20] and the Feb 2011 VRBPAC report [21]. We queried the Influenza Research Database [22] and the EpiFlu Database [23] for HA nucleotide sequences by matching strain names, e.g. A/HongKong/1/1968, and only strains for which sequence was present was retained. If a strain had multiple sequences in the databases we preferentially kept the IRD sequence and preferentially kept the longest sequence in IRD. This dataset had 2051 influenza isolates (present as either virus or serum in HI comparisons) dating from 1968 to 2011. However, the majority of isolates were present from 2002 to 2007. Because we are interested in longer-term antigenic evolution, we censored the data to have at most 20 virus isolates per year, preferentially keeping those isolates with more antigenic comparisons. We then kept only those serum isolates that are relatively informative to the antigenic placement of viruses, dropping serum isolates that are compared to 4 or fewer different virus isolates. This censoring left 429 virus isolates, 519 serum isolates and 10,097 HI measurements.

Antigenic data for influenza A (H1N1) was collected from previous publications [5, 13, 24–37] and NIMR vaccine strain selection reports for 2002–2010 [14–17, 38–46]. The same procedure was followed as was followed for H3N2 to match sequence data and to censor antigenic comparisons. This procedure yielded 124 virus isolates, 77 serum isolates and 1882 HI measurements over the course of 1977 to 2009.

Antigenic comparisons for influenza B Victoria-lineage were collated from previous publications [5] [Include in BibTex: Ansaldi04, AusWHO06, Barr06, Daum06, Lin07, Muyanga01, Puzelli04, Rota90, Shaw02, Xu04] and NIMR vaccine strain selection reports for 2002–2012 [14–20, 38–45, 47, 48]. Here, the sequence matching and censoring procedure yielded 179 virus isolates, 70 serum isolates and 2003 HI measurements over the course of 1986 to 2011.

Antigenic comparisons for influenza B Yamagata-lineage were collected from previous publications [5] [Include in BibTex: Abed03, Ansaldi03, Ansaldi04, AusWHO06, Barr06, Daum06, Kanegae90, Lin07, Matsuzaki04, Muyanga01, Nakagawa02, Nakajima92, Nerome98, Puzelli04, Rota90, Shaw02, Xu04] and NIMR vaccine strain selection reports for 2002–2012 [14–20, 38–45, 47, 48]. For B/Yamagata, the matching and censoring procedure resulted in 174 virus isolates, 69 serum isolates and 1962 HI measurements over the course of 1987 to 2011.

Sequences were aligned using MUSCLE v3.7 under default parameters [49].

Acknowledgments

Funding

References

1. WHO (2009) Influenza Fact sheet. Available at http://www.who.int/mediacentre/factsheets/fs211/en/.
2. Rota P, Hemphill M, Whistler T, Regnery H, Kendal A, et al. (1992) Antigenic and genetic characterization of the haemagglutinins of recent cocirculating strains of influenza B virus. The Journal of general virology 73: 2737.
3. Nelson MI, Holmes EC (2007) The evolution of epidemic influenza. Nat Rev Genet 8: 196–205.
4. Hirst G (1943) Studies of antigenic differences among strains of influenza A by means of red cell agglutination. J Exp Med 78: 407–423.
5. Hay, AJ and Gregory, V and Douglas, AR and Lin, YP (2001) The evolution of human influenza viruses. Phil Trans R Soc Lond B 356: 1861–1870.
6. Smith DJ, Lapedes AS, de Jong JC, Bestebroer TM, Rimmelzwaan GF, et al. (2004) Mapping the antigenic and genetic evolution of influenza virus. Science 305: 371–376.

7. Fitch WM, Bush RM, Bender CA, Cox NJ (1997) Long term trends in the evolution of H(3) HA1 human influenza type A. Proc Natl Acad Sci USA 94: 7712-8.

8. Russell CA, Jones TC, Barr IG, Cox NJ, Garten RJ, et al. (2008) The global circulation of seasonal influenza A (H3N2) viruses. Science 320: 340–346.

9. Lemey P, Rambaut A, Welch J, Suchard M (2010) Phylogeography takes a relaxed random walk in continuous space and time. Mol Biol Evol 27: 1877–1885.

10. Cai Z, Zhang T, Wan XF (2010) A computational framework for influenza antigenic cartography. PLoS Comput Biol 6: e1000949.

11. Oh M, Raftery A (2001) Bayesian multidimensional scaling and choice of dimension. Journal of the American Statistical Association 96: 1031–1044.

12. Drummond AJ, Rambaut A (2007) BEAST: Bayesian evolutionary analysis by sampling trees. BMC Evol Biol 7: 214.

13. Barr I, McCauley J, Cox N, Daniels R, Engelhardt O, et al. (2010) Epidemiological, antigenic and genetic characteristics of seasonal influenza A (H1N1), A (H3N2) and B influenza viruses: basis for the WHO recommendation on the composition of influenza vaccines for use in the 2009-2010 Northern Hemisphere season. Vaccine 28: 1156–1167.

14. Hay AJ, Lin YP, Gregory V, Bennet M (2002) Annual Report. Technical report, WHO Collaborating Centre for Reference and Research on Influenza, National Institute for Medical Research, UK.

15. Hay A, Daniels RS, Lin YP, Zheng X, Gregory V, et al. (March 2008) Characteristics of human influenza AH1N1, AH3N2, and B viruses isolated September 2007 to February 2008. Technical report, WHO Collaborating Centre for Reference and Research on Influenza, National Institute for Medical Research, UK.

16. Hay A, Daniels RS, Lin YP, Zheng X, Hou T, et al. (Feb 2009) Antigenic and genetic characteristics of human influenza A(H1N1), A(H3N2) and B viruses isolated during October 2008 to February 2009. Technical report, WHO Collaborating Centre for Reference and Research on Influenza, National Institute for Medical Research, UK.

17. McCauley J, Daniels R, Lin YP, Zheng X, Hou T, et al. (Feb 2010) Report prepared for the WHO annual consultation on the composition of influenza vaccine for the Northern Hemisphere. Technical report, WHO Collaborating Centre for Reference and Research on Influenza, National Institute for Medical Research, UK.

18. McCauley J, Daniels R, Lin YP, Zheng X, Hou T, et al. (Sep 2010) Report prepared for the WHO annual consultation on the composition of influenza vaccine for the Southern Hemisphere. Technical report, WHO Collaborating Centre for Reference and Research on Influenza, National Institute for Medical Research, UK.

19. McCauley J, Daniels R, Lin YP, Zheng X, Gregory V, et al. (Sep 2011) Report prepared for the WHO annual consultation on the composition of influenza vaccine for the Southern Hemisphere. Technical report, WHO Collaborating Centre for Reference and Research on Influenza, National Institute for Medical Research, UK.

20. McCauley J, Daniels RS, Lin YP, Zheng X, Gregory V, et al. (Feb 2012) Report prepared for the WHO annual consultation on the composition of influenza vaccine for the Northern Hemisphere. Technical report, WHO Collaborating Centre for Reference and Research on Influenza, National Institute for Medical Research, UK.

21. Cox NJ (Feb 2011) Information for the Vaccines and Related Biological Products Advisory Committee. Seasonal Influenza Vaccines. Technical report, WHO Collaborating Centre for Surveillance, Epidemiology and Control of Influenza, Centers for Disease Control and Prevention, USA.

22. Squires R, Noronha J, Hunt V, García-Sastre A, Macken C, et al. (2012) Influenza research database: an integrated bioinformatics resource for influenza research and surveillance. Influenza and Other Respiratory Viruses DOI: 10.1111/j.1750-2659.2011.00331.x.

23. Bogner P, Capua I, Lipman D, Cox N, et al. (2006) A global initiative on sharing avian flu data. Nature 442: 981–981.

24. Kendal AP, Noble GR, Skehel JJ, Dowdle WR (1978) Antigenic similarity of influenza A(H1N1) viruses from epidemics in 1977–1978 to Scandinavian strains isolated in epidemics of 1950–1951. Virology 89: 632–636.

25. Webster R, Kendal A, Gerhard W (1979) Analysis of antigenic drift in recently isolated influenza A (H1N1) viruses using monoclonal antibody preparations. Virology 96: 258–264.

26. Nakajima K, Nakajima S, Nerome K, Takeuchi Y, Sugiura A, et al. (1979) Genetic relatedness of some 1978–1979 influenza H1N1 strains to 1953 H1N1 strain. Virology 99: 423–426.

27. Nakajima S, Cox NJ, Kendal AP (1981) Antigenic and genomic analyses of influenza A(H1N1) viruses from different regions of the world, February 1978 to March 1980. Infection and Immunity 32: 287–294.

28. Chakraverty P, Cunningham P, Pereira MS (1982) The return of the historic influenza A H1N1 virus and its impact on the population of the United Kingdom. The Journal of Hygiene 89: 89–100.

29. Pereira MS, Chakraverty P (1982) Influenza in the United Kingdom 1977–1981. Epidemiology & Infection 88: 501–512.

30. Chakraverty P, Cunningham P, Shen GZ, Pereira MS (1986) Influenza in the United Kingdom 1982–85. The Journal of Hygiene 97: 347–358.

31. Cox NJ, Bai ZS, Kendal AP (1983) Laboratory-based surveillance of influenza A(H1N1) and A(H3N2) viruses in 1980–81: antigenic and genomic analyses. Bulletin of the World Health Organization 61: 143–152.

32. Daniels RS, Douglas AR, Skehel JJ, Wiley DC (1985) Antigenic and amino acid sequence analyses of influenza viruses of the H1N1 subtype isolated between 1982 and 1984. Bulletin of the World Health Organization 63: 273–277.

33. Raymond F, Caton A, Cox N, Kendal A, Brownlee G (1986) The antigenicity and evolution of influenza H1 haemagglutinin, from 1950–1957 and 1977–1983: Two pathways from one gene. Virology 148: 275–287.

34. Stevens DJ, Douglas AR, Skehel JJ, Wiley DC (1987) Antigenic and amino acid sequence analysis of the variants of H1N1 influenza virus in 1986. Bulletin of the World Health Organization 65: 177–180.

35. Donatelli I, Campitelli L, Ruggieri A, Castrucci MR, Calzoletti L, et al. (1993) Concurrent antigenic analysis of recent epidemic influenza A and B viruses and quantitation of antibodies in population serosurveys in Italy. European Journal of Epidemiology 9: 241–250.

36. Daum LT, Canas LC, Smith CB, Klimov A, Huff W, et al. (2002) Genetic and Antigenic Analysis of the First A/New Caledonia/20/99-like H1N1 Influenza Isolates Reported in the Americas. Emerging Infectious Diseases 8: 408–412.

37. McDonald NJ, Smith CB, Cox NJ (2007) Antigenic drift in the evolution of H1N1 influenza A viruses resulting from deletion of a single amino acid in the haemagglutinin gene. Journal of General Virology 88: 3209–3213.

38. Hay AJ, Lin YP, Gregory V, Bennet M (2003) Annual Report. Technical report, WHO Collaborating Centre for Reference and Research on Influenza, National Institute for Medical Research, UK.

39. Hay AJ, Lin YP, Gregory V, Bennet M (2004) Annual Report. Technical report, WHO Collaborating Centre for Reference and Research on Influenza, National Institute for Medical Research, UK.

40. Hay AJ, Lin YP, Gregory V, Bennet M (Feb 2005) Characteristics of human influenza A H1N1, A H3N2 and B viruses isolated October 2004 to January 2005. Technical report, WHO Collaborating Centre for Reference and Research on Influenza, National Institute for Medical Research, UK.

41. Hay AJ, Lin YP, Gregory V, Bennet M (Sep 2005) Characteristics of human influenza AH1N1, AH3N2 and B viruses isolated February to July 2005. Technical report, WHO Collaborating Centre for Reference and Research on Influenza, National Institute for Medical Research, UK.

42. Hay AJ, Lin YP, Gregory V, Bennet M (March 2006) Characteristics of human influenza AH1N1, AH3N2 and B viruses isolated October 2005 to February 2006. Technical report, WHO Collaborating Centre for Reference and Research on Influenza, National Institute for Medical Research, UK.

43. Hay AJ, Lin YP, Gregory V, Bennet M (Sep 2006) Characteristics of human influenza AH1N1, AH3N2 and B viruses isolated January to September 2006. Technical report, WHO Collaborating Centre for Reference and Research on Influenza, National Institute for Medical Research, UK.

44. Hay AJ, Daniels R, Lin YP, Zheng X, Gregory V, et al. (March 2007) Characteristics of human influenza AH1N1, AH3N2 and B viruses isolated September 2006

to February 2007. Technical report, WHO Collaborating Centre for Reference and Research on Influenza, National Institute for Medical Research, UK.

45. Hay AJ, Daniels R, Lin YP, Zheng X, Gregory V, et al. (Sep 2007) Characteristics of human influenza AH1N1, AH3N2 and B viruses isolated February to August 2007. Technical report, WHO Collaborating Centre for Reference and Research on Influenza, National Institute for Medical Research, UK.

46. Hay AJ, Daniels R, Lin YP, Zheng X, Hou T, et al. (Sep 2008) Characteristics of human influenza AH1N1, AH3N2, and B viruses isolated February to August 2008. Technical report, WHO Collaborating Centre for Reference and Research on Influenza, National Institute for Medical Research, UK.

47. Hay A, Daniels R, Lin YP, Zheng X, Hou T, et al. (Sep 2009) Antigenic and genetic characteristics of pandemic A(H1N1) viruses and seasonal A(H1N1), A(H3N2) and B viruses isolated during February to August 2009. Technical report, WHO Collaborating Centre for Reference and Research on Influenza, National Institute for Medical Research, UK.

48. McCauley J, Daniels R, Lin YP, Zheng X, Gregory V, et al. (Feb 2011) Report prepared for the WHO annual consultation on the composition of influenza vaccine for the Northern Hemisphere. Technical report, WHO Collaborating Centre for Reference and Research on Influenza, National Institute for Medical Research, UK.

49. Edgar RC (2004) MUSCLE: multiple sequence alignment with high accuracy and high throughput. Nucleic Acids Res 32: 1792–1797.

Supporting Information